SAND2021-11801C

Sensitivity Analysis of Moving Packed-Bed Heat Exchanger Models

Christopher P. Bowen[1, a)] and Kevin J. Albrecht[1]

[1]*Concentrating Solar Technologies, Sandia National Laboratories, 1515 Eubank Blvd. SE, Albuquerque, NM 87123, USA*

[a)] Corresponding author: cpbowen@sandia.gov

Abstract. A sensitivity analysis of moving packed-bed heat exchanger models is presented. A heat exchanger symmetric half-plate geometry based on the Gen 3 Particle Pilot Plant (G3P3) is meshed and solved using a conjugate heat transfer model. Seven independent variables are sampled at random within prescribed limits and the model is run for up to 64 different combinations of the input parameters. The overall heat transfer coefficient is output for each simulation and the Sobol index is calculated and used to compare sensitivity levels of the inputs. The analysis is performed in two parts to provide insight from both an overall design and optimization perspective in addition to an operational standpoint for an existing heat exchanger. The first key finding is that the overall heat transfer coefficient sensitivity is almost entirely dominated by the particle channel width. The second insight is that for an existing heat exchanger where the geometric parameters are fixed, the overall heat transfer coefficient prediction still has a significant level of uncertainty that can be limited by better characterizing the packed-bed void fraction.

INTRODUCTION

Solid particles have emerged as a promising candidate for next generation concentrating solar power (CSP) systems due to their favorable solar absorption properties and potential as an efficient heat-transfer fluid. While on-sun testing has shown that particles can be efficiently irradiated and heated to temperatures in excess of 700 °C, advances in the particle-to-sCO_2 heat transfer process are needed to achieve levelized cost of electricity (LCOE) targets. A significant contributor to the overall cost of a CSP heat exchanger is the raw material, a factor which can be minimized by maximizing the overall heat transfer coefficient. A design study by Ho et al. [1] performed a cost-performance analysis of three particle heat exchanger designs proposed by industry sources for use in a 100 kW_t system. The authors determined that a shell-and-plate moving packed bed design would provide a sufficient heat transfer coefficient while minimizing manufacturing complexity and cost. In partnership with Vacuum Process Engineering and Solex Energy Science a counter crossflow prototype heat exchanger was developed and tested at Sandia's National Solar Thermal Test Facility (NSTTF). Albrecht et al. [2] used a 3-D FEA model to simulate the exchanger performance and reported that the experimentally measured heat transfer coefficients were approximately a factor of 2 lower than the modelled values. Computational models are necessary for developing heat exchanger designs in a time and cost-effective manner, but significant deviation between the model output and experimentally realized performance presents a significant source of risk for implementation at MW_t scales. In this work, a sensitivity analysis is performed using a 3-D FEA model to determine the Sobol indices between selected geometric and fluid-thermal particle flow properties and the predicted overall heat transfer coefficients in a shell-and-plate moving packed bed heat exchanger design. The results provide insights into the physical design considerations and identify first order variables for which uncertainty must be limited to improve the accuracy and reliability of the model.

SENSITIVITY STUDY OBJECTIVES

The objective of this study is to determine which variables in a moving packed-bed particle-to-sCO_2 heat exchanger design have a first order effect on the overall heat transfer coefficient (U). First, a sensitivity analysis is conducted in which two geometric parameters and five thermal-fluid properties in a moving packed bed model are sampled over the ranges provided in Table 1. The results of any variance-based sensitivity analysis can be highly dependent on the sampled ranges of each independent variable, and thus it is critical that the values in Table 1 be carefully defined based on realistic expected values. The range of 2-6 mm for the particle channel width is limited on the low end by the necessity to avoid particle bridging and on the high end by excessive conductive thermal resistance. The lower sCO_2 channel diameter limit of 0.75 mm was selected based on typical constraints in the microchannel etching processes while also considering the sCO_2 pressure drop across each channel. The upper limit of 2.5 mm fits inside the predetermined plate thickness (3.175 mm) while not exceeding mechanical stress limits at the desired operating conditions. Albrecht et al. [3] developed a 1-D moving packed bed heat exchanger model in order to determine an optimal design basis for use in next-generation CSP plants. Their 1-D model employed the same relationships used in this effort for determining the packed-bed conductivity as a function of particle emissivity (ε_p), particle diameter (d_p), and particle void fraction (VF). The sampling range for each of those three variables was informed from the results of that analysis.

The final two variables, flow non-uniformity in both the moving packed-bed and the sCO_2 microchannels are largely unexplored in the literature. While the heat exchanger and system hardware are designed with flow uniformity in mind for both the packed-bed and the microchannels, at temperature these physics are difficult to predict and flow maldistributions in either domain are likely to occur. The packed-bed non-uniformity parameter (NP_{pb}) is defined in Equation 1 such that a linear velocity distribution is established across the length of the channel with a matched mean velocity ($\overline{V}$) that maintains a constant particle flow rate. There is no variation in the profile with respect to the channel width. The minimum value of $NP_{pb} = 0$ creates a uniform flow, while $NP_{pb} = 1$ creates a linear profile with maximum velocity double the minimum velocity. Similarly, the sCO_2 non-uniformity parameter (NP_{CO2}) is defined such that $NP_{CO2} = 0$ distributes the total sCO_2 flow rate evenly among the channels, while $NP_{CO2} = 1$ distributes the total flow linearly such that the mass flow at one of the end channels is double that of the opposing end channel. A negative value of NP_{CO2} simply changes which side receives the augmented mass flow. This was included to analyze if there is an effect on the heat transfer performance if the flow deficits in the packed-bed and sCO_2 channels present themselves on the same or opposite sides.

Comparing the sensitivities of both the geometric and fluid-thermal variables provides insight into heat exchanger performance from a design standpoint. Once a heat exchanger is built, however, the geometric parameters are fixed and the uncertainty in the performance is dictated by the fluid-thermal variables. If the measured heat transfer

TABLE 1. Variables included in the sensitivity study and the minimum and maximum values bounding the sampling range for each.

Variable	Minimum Value	Maximum Value
Particle channel width	2 mm	6 mm
Microchannel diameter	0.75 mm	2.5 mm
Packed-bed void fraction (VF)	0.37	0.55
Particle diameter (d_p)	100 µm	600 µm
Particle emissivity (ε_p)	0.7	1.0
Packed-bed non-uniformity parameter (NP_{pb})	0	1.0
sCO_2 non-uniformity parameter (NP_{CO2})	-1.0	1.0

$$V_{min} = \frac{\overline{V}}{\left(1 + 0.5NP_{pb}\right)} \rightarrow V_{max} = 2\overline{V} - V_{min} \#(1)$$

performance during operation varies from the model prediction, understanding which fluid-thermal properties have the highest degree of correlation with the model output is important. This insight might allow for altering of particular elements of the system design to decrease variance in the performance. It could also motivate engineers to implement targeted instrumentation to better characterize the model inputs to decrease the uncertainty in the model. A reduction in model uncertainty would mitigate the need to overdesign future heat exchanger designs, saving material costs and reducing the LCOE. To isolate the effects of the fluid-thermal variables, a separate sensitivity analysis is performed for a heat exchanger with fixed particle channel width and microchannel diameter.

THERMAL MODEL AND SENSITIVITY METHODOLOGY

The present study models a shell-and-plate moving packed-bed counterflow heat exchanger designed by Sandia, Solex, and VPE for future implementation in the G3P3 project. The heat exchanger consists of 32 full plates and a half plate on each end. In the nominal design, each plate has an active heat transfer surface area that is 1.258 m tall by 0.61 m wide and is formed by diffusion bonding two 3.175 mm thick plates each consisting of a fixed number of etched microchannels. At the design operating conditions listed in Table 2, the overall thermal duty of the heat exchanger is expected to be 1 MW_t.

Due to computational constraints, the modeled geometry is simplified to a single half-plate as shown in the images in Fig. 1. It is assumed that potential variations across the heat exchanger plates as well as potential edge effects at the end walls are negligible. Since the geometry is a half-plate, the modeled plate thickness (3.175 mm) is half of the full plate thickness (6.35 mm). Similarly, the modeled packed-bed channel width is half (1-3 mm) of the of the prescribed full-plate value (2-6 mm). Symmetry boundaries are enforced on the outer surfaces of both the plate domain (depicted in grey) as well as the packed-bed domain (depicted in red). In the right image of Fig. 1, a full plate geometry is illustrated. The symmetry planes are marked with dotted black lines and the modeled section is shown in color while the unmodeled half is in faded black and white. In accordance with the assumption of uniformity, the total particle and sCO_2 mass flow rates from Table 2 are divided by 66 (33 plates or 66 half-plates) to determine the flow rates in the truncated domain. Each conjugate simulation is solved using the Sandia FEA thermal solver SIERRA Aria [4]. The packed-bed is treated as a continuum with temperature dependent composite thermophysical properties for CARBO HSP 40/70 particles. The continuum assumption is commonly made to avoid higher-fidelity granular flow modeling. At the inlet of the packed-bed domain, labeled in Fig. 1, a velocity distribution is enforced based on the particle flow rate through the half-channel and the value of NP_{pb} for the simulation as calculated by Equation 1. The inlet temperature is set to 775 °C in accordance with Table 2. At the particle-wall interface, the symmetry boundary enforces a slip condition such that the prescribed velocity distribution at the inlet of the packed-bed is retained through the height of the channel. A steady state advection-diffusion energy solver is used to solve for the temperature distribution through the packed-bed.

At the particle-wall interface, the wall normal heat fluxes into the plate wall elements are interpolated from the nearest packed-bed wall elements. The plate region is assigned a conductivity of Inconel 617 which is a candidate nickel-alloy material capable of operating at the required pressures and temperatures.

The sCO_2 microchannels are approximated as perfect semi-circles, and a 1-D advective bar approach is implemented rather than meshing and resolving the sCO_2 fluid. Accurately resolving the turbulent boundary layer fluxes of sCO_2 microchannel flow using traditional Reynolds-Averaged Navier Stokes turbulence models typically requires non-dimensional wall distances (y+) below unity as demonstrated by Kruizenga et al. [5]. The authors showed that traditional turbulent wall functions significantly overestimate the wall heat flux when compared to established turbulent heat transfer correlations. Fully resolving the boundary layer into the viscous sublayer requires prohibitive mesh cell counts and computational run time. In the 1-D advective bar approach a bar line element runs down the center of each channel as shown by the yellow lines in the right image of Fig. 1. Each bar is discretized by 50 equidistant nodes. A fraction of the total mass flow rate for the half plate is assigned at the inlet node of each bar depending on the value of NP_{CO2} for the given simulation. The inlet temperature is set to 565 °C at each inlet node

Table 2: G3P3 Heat exchanger design point operating conditions

Particle Inlet Temperature	sCO_2 Inlet Temperature	Particle Flow Rate	sCO_2 Flow Rate	sCO2 Pressure
775 °C	565 °C	5.03 kg/s	5.26 kg/s	25 MPa

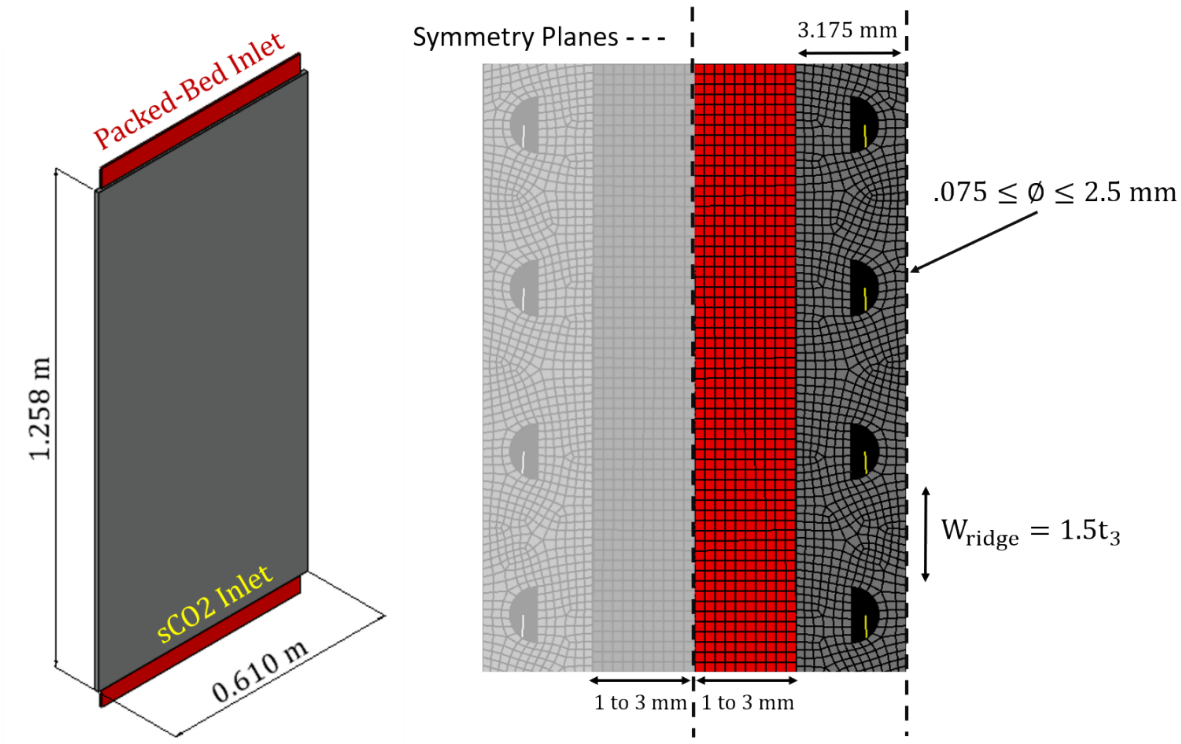

FIGURE 1. Heat exchanger half-plate computational domain (left) and top down mesh-view with fixed and parametric dimensions (right).

in accordance with the operating conditions listed in Table 2. A 1-D advection solver is used to calculate the temperature change along the bar, and the fluid density, specific heat, and viscosity are updated as a function of temperature. Changes in these properties consequently change the channel Reynolds number values. At each node, the corresponding Reynolds numbers are used to calculate a Nusselt number using the standard Gnielinski correlation [6]. The wall heat transfer coefficient is then calculated, which is used to set the wall flux boundary condition at the sCO_2-wall interface.

The sensitivity study is performed using the Sandia native code DAKOTA [7] using a Latin-Hypercube Sampling (LHS) approach. The total number of simulations (N) to run is first prescribed, and each variable range is divided into N uniformly distributed intervals. For every simulation, each independent variable is randomly assigned a value with a new interval. By using a unique interval in each simulation, the LHS method ensures that the full range is sufficiently sampled. This can reduce the number of samples needed for statistical convergence compared to a traditional Monte Carlo approach in which random samples are selected over the range without any consideration of the previously generated sample points.

After assigning the random variables to each simulation, the geometry and mesh for each is first generated using Sandia's native meshing toolkit Cubit. Each plate has the same general footprint (1.258 x 0.61 x 0.003175 m) as shown in Fig. 1. The flat face of each microchannel lies along the mid-thickness line of the plate. The total number of microchannels etched in each plate is maximized while also considering ASME allowable stress limitations for pressure containment at temperature. In general, it is desirable from a heat transfer perspective to include as many microchannels as possible, however, reducing the material in the ridge between the channels increases the membrane stresses in the ridges. To ensure each geometry created is a mechanically viable design in practice, the required ridge width is calculated using the equations and guidelines for printed circuit heat exchangers detailed by Pierres et al. [8]. The simplified block geometry schematic published by the authors is provided in Fig. 2 for reference. The authors state that the membrane stress must be smaller than SE, where S is the design stress and E is the joint factor (0.7 for a diffusion bonded block). At the design operating pressure (28 MPa) and temperature (800 °C), the design stress for IN617 is 31.3 MPa according to the ASME Boiler and Pressure Vessel Code [9]. The minimum ridge width (t_3) is calculated using the equation in Fig. 2 where P is the design pressure and h is the channel diameter. An additional safety factor of 1.5 was added to the original formulation provided by Pierres et al. The side margin or edge thickness

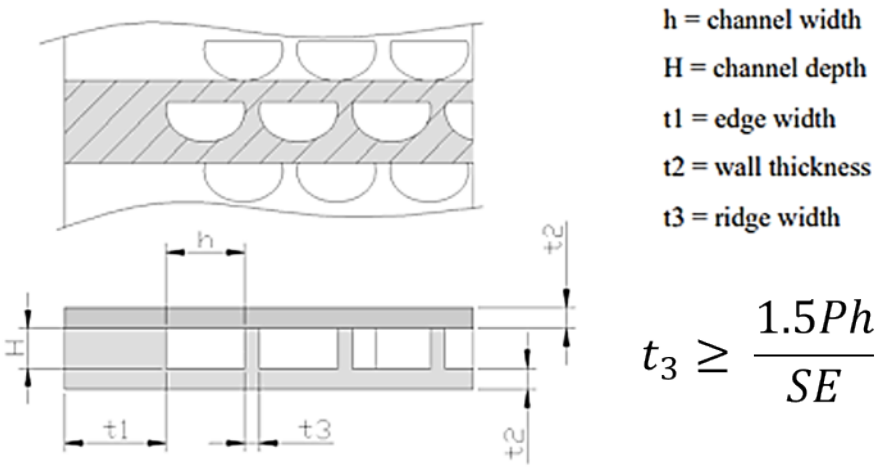

FIGURE 2. Simplified printed circuit heat exchanger block geometry for mechanical design by Pierres et al. [8].

(t_1) is set to 15 mm, which provides a minimum safety factor of 1.5 when the microchannel diameter is a maximum of 2.5 mm. Subtracting the side margins from the plate width, the maximum number of microchannels that fit in the remaining space with the required ridge width (t_3) is determined. The side margins are extruded past the plate at a distance equal to the particle channel half-width for the given simulation, creating the containing walls for the packed-bed. The packed-bed domain is generated and contained within the plate and side containing walls but extends 0.05 m past the top and bottom plate edges. This is done strictly for postprocessing and visualization purposes, and the extended header sections are treated adiabatically. It is noted that the minimum wall thickness (t_2) that occurs for a microchannel diameter of 2.5 mm results in a safety factor of 1.

The required dimensions are sent to a Cubit algorithm which generates the conjugate domain and then creates a hexahedral mesh. The base size of the elements in the packed-bed domain is set to 1/10 of the half-channel width to ensure 10 elements span the channel. In the plate domain, a base size of 1/7 of the microchannel diameter is used. While this creates a mesh density that exceeds the requirements to solve a simple conduction problem, the refinement is needed to prevent truncation or distortion of the microchannels during the meshing process. The total element count is a function of the geometric settings for each simulation.

An input file for the Sierra Aria simulation is then generated to execute the solver. The boundary conditions and thermophysical properties in each of the three domains are assigned as formerly described. The non-uniformity parameters dictate the inlet flow conditions in both the packed-bed and sCO_2 domains. The remaining three variables VF, d_p, and ε_p each factor into the calculation for the packed-bed effective conductivity and particle-wall contact resistance, which is calculated using a correlation developed by Zehner, Bauer, and Schlünder (ZBS) [10]. The ZBS model is implemented using temperature dependent thermal-fluid properties for the HSP 40/70 particles and surrounding air, such that every element is assigned a unique conductivity that is a function of the local temperature, VF, d_p, and ε_p. The steady state solver is run for each simulation and an energy balance is monitored to verify each is fully converged. Fig. 3 shows velocity contours for both the packed-bed and sCO_2 advective bar solutions for a particular simulation where $NP_{pb} = 0.83$ and $NP_{CO2} = -0.753$. The steep velocity gradients in each domain are apparent and the faster flow in the sCO_2 channels overlaps with the slower flow in the packed-bed. Figure 4 provides steady state thermal contours as seen from the exposed packed-bed symmetry plane (left), the plate symmetry plane (middle), and for the advective bar elements (right). In regions of the packed-bed with faster flowing particles, the decreased residence time results in less heat loss and thus a lateral gradient emerges in addition to the expected streamwise gradient. A similar gradient occurs in both the plate and sCO_2 flow due to both the hotter particle temperatures and the augmented heat transfer coefficients in the regions of the packed-bed with higher particle velocities.

POST-PROCESSING AND SENSITIVITY CALCULATIONS

The overall heat transfer coefficient (U) is calculated for each steady state solution using the standard counterflow heat exchanger formulation in Equation 2 where the total heat transfer to the sCO_2 is calculated by summing the enthalpy addition of each individual microchannel. The model outputs are passed back to DAKOTA, and variance-

$$\sum_{0}^{CO_2.ch} \dot{m}_{CO_2.ch} \int_{CO_2,in}^{CO_2,out} C_p dT = UA \left[\frac{(T_{pb,in} - T_{CO_2,out}) - (T_{pb,out} - T_{CO_2,in})}{\ln\left(\frac{T_{pb,in} - T_{CO_2,out}}{T_{pb,out} - T_{CO_2,in}}\right)} \right] \#(2)$$

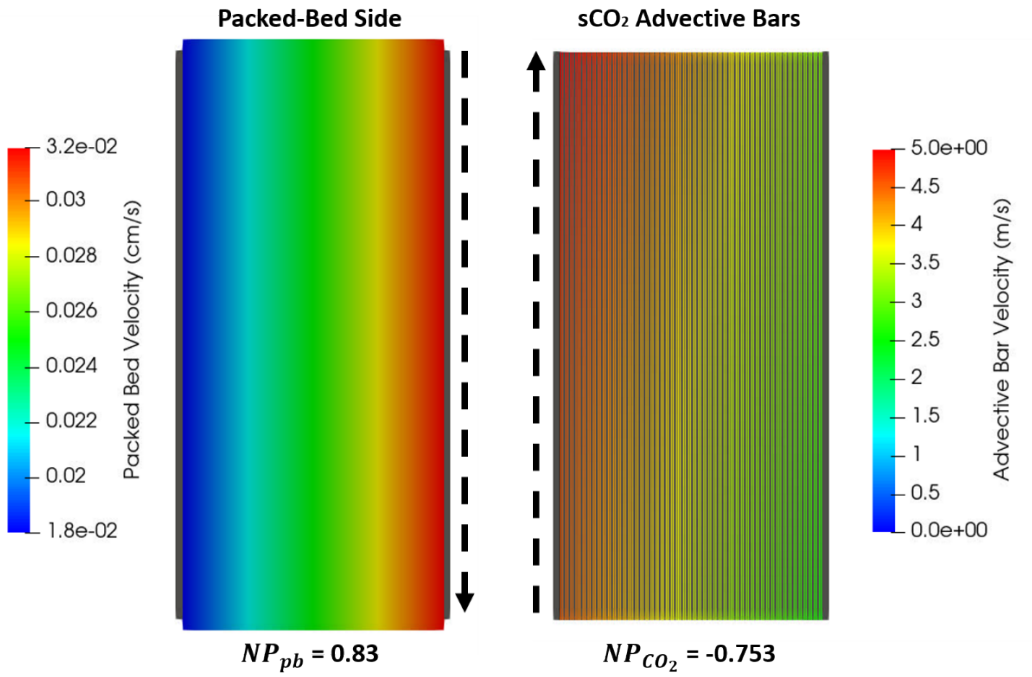

FIGURE 3. Packed-bed (left) and sCO_2 advective bar (right) velocity contours for case with high flow non-uniformities.

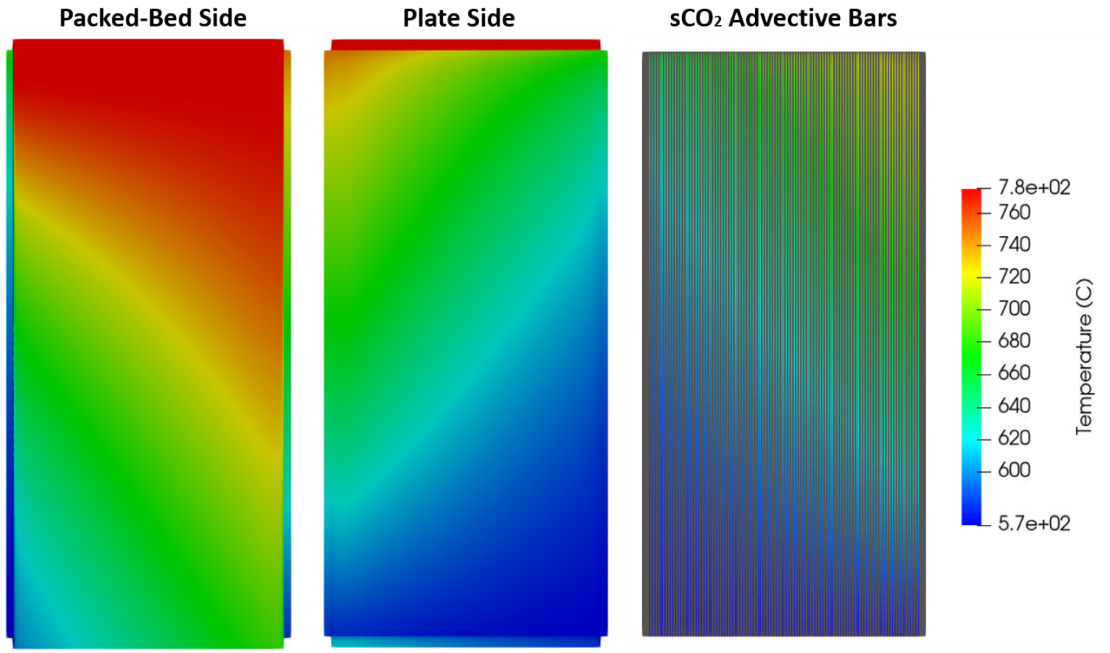

FIGURE 4. Packed-bed (left), plate (center), and sCO_2 advective bar (right) temperature contours for the same case as Fig. 3.

based sensitivity analysis is used to calculate the Sobol index for each independent variable. This metric gives a comparative measure of how much of the output variance is caused by variance in each individual input and can be interpreted as a percent sensitivity of an output to a given input. A Sobol index is also calculated for interactions between the various combinations of independent variables. The first order Sobol indices and second order interactions should sum to unity for a given set of data.

Calculating statistically converged Sobol indices directly from the simulation outputs would require an excessive number of samples. Saltelli et al. [11] approximated that the number of samples required for a variance-based sensitivity study to reach convergence is $n \times (M+2)$ where $M$is the number of independent variables and n is a factor that varies depending on the complexity of the model. Typically, $n > 1000$, so reaching convergence could take upwards of 10,000 model evaluations, which is impractical for this study. To circumvent these constraints, surrogate models are often built from sparse sets of training data and used to sample a more robust set of data. Polynomial Chaos Expansion (PCE) is one of these surrogate modeling methods and is chosen to approximate the Sobol indices in this model. The advantage of the PCE method is it first uses a polynomial expansion to approximate the model, and then directly calculates the Sobol indices from that expansion. The model does not need require re-sampling and thus is computationally efficient. The details of the PCE approach are available in the DAKOTA reference manual [7]. Although PCE performs the variance-based decomposition analytically, the polynomial expansion surrogate model will become more accurate and converge when provided additional training data. A common approach is to begin with a number of samples roughly equal to the number of inputs and double the number of samples until the Sobol indices converge. For this sensitivity study 16, 32, and 64 model evaluations are executed. It was found that the variables that showed non-negligible sensitivity (Sobol index ≥ 0.01) had less than a 5% change in the Sobol index between 32 and 64 simulation evaluations.

The overall heat transfer coefficient (U) is plotted against each independent variable in Fig. 5 for the 64-sample evaluation. Above each plot, the Sobol index (S_i) is also provided. The results indicate the heat exchanger performance is primarily dictated by its geometric design, as the particle channel width and microchannel diameter account for over 83% of the variance of U. The particle channel width is alone responsible for approximately 80% of the variance and is the only data that shows a clear and nearly monotonic relationship. The increase in width from 2-6 mm causes an approximate 60% reduction in the heat transfer coefficient. The comparatively low Sobol index for microchannel diameter is due in large part to the operating conditions, which are designed to realize high heat transfer coefficients that are not as easily achieved in the packed-bed flow. The majority of the overall thermal resistance in the heat exchanger is contributed from the packed-bed, and thus variations in the sCO_2 side are relatively minor in comparison. The packed-bed void fraction is the only fluid-thermal variable of measurable importance, and accounts for 12% of the variance in the output. These results confirm the previous finding of Albrecht et al. [3] that the overall heat transfer coefficient is most sensitive to changes in the bed channel width, and to a lesser degree the packed-bed void fraction.

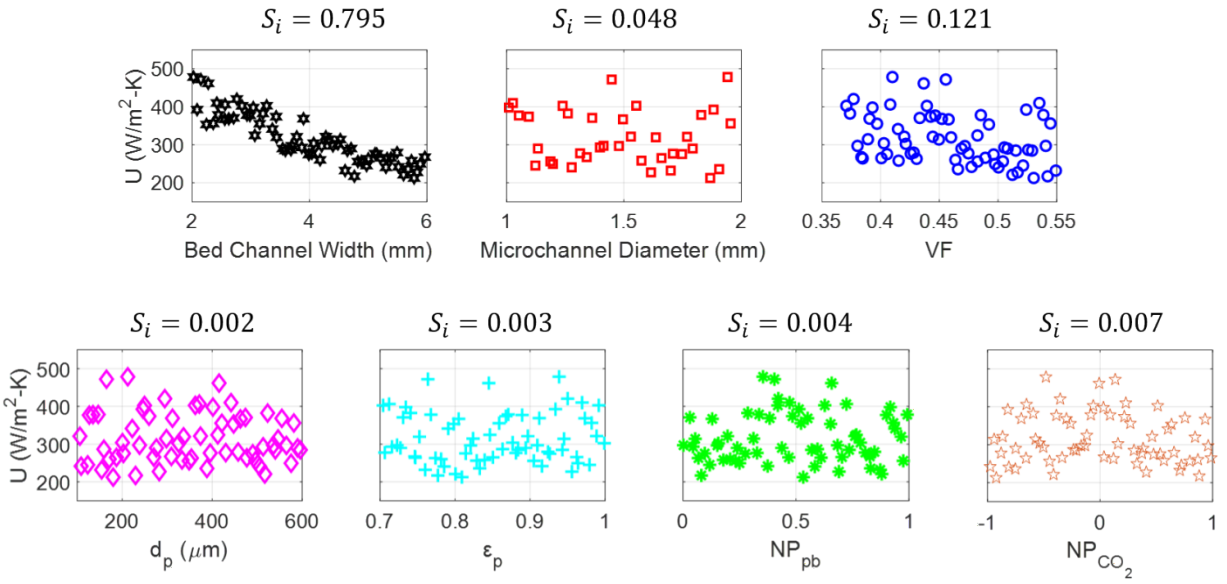

FIGURE 5. U vs sensitivity variables for 64-sample evaluation.

From a design optimization standpoint, the results shown in Fig. 5 suggest that only three variables dictate the performance of a moving packed-bed heat exchanger. In practice, however, once a heat exchanger is designed and built, the particle channel width is fixed. The sensitivity in the performance during operation will naturally be less pronounced, but this variability due to the fluid-thermal variables is still of interest. A second study was performed where the particle channel width and microchannel diameter were excluded as independent variables. The former was assigned a constant value of 3 mm and the latter a constant equal to 0.9 mm, matching the original G3P3 design. The same ranges of variables were sampled 64 times using the same LHS technique, and the results were postprocessed in the same manner. The output scatter plots, and corresponding S_i values are provided in Fig. 6. The bottom plot in the figure provides a histogram of the output values with a normal probability density function fit to it. All of the data to the right of the blacked dashed line is in the single-sided 95% tolerance interval. The first important observation from this plot is that the range of heat transfer coefficients in which there is 95% certainty spans over 100 W/m^2-K. While this is notably less than the range in the full sensitivity study, it still represents about 33% of the total heat transfer and is certainly non-negligible. The void fraction accounts for approximately 57.6% of the variance, while the particle diameter and emissivity account for only 12%. About 70% of the sensitivity for an operating heat exchanger of fixed dimension is controlled by the packed-bed conductivity variables in the ZBS correlation. The remaining 30% is due to potential variation in the particle and sCO_2 flow distributions in roughly equal proportion. The non-uniformity scatter plots show a slight trend with NP_{CO2}. It appears that U increases with NP_{CO2} up to $NP_{CO2} = 0$, at which point it levels off. This suggests that having particle and sCO_2 non-uniformities that result in augmented particle flow rates over plate regions with lower sCO_2 mass flow could compromise the performance. On the other hand, it suggests that

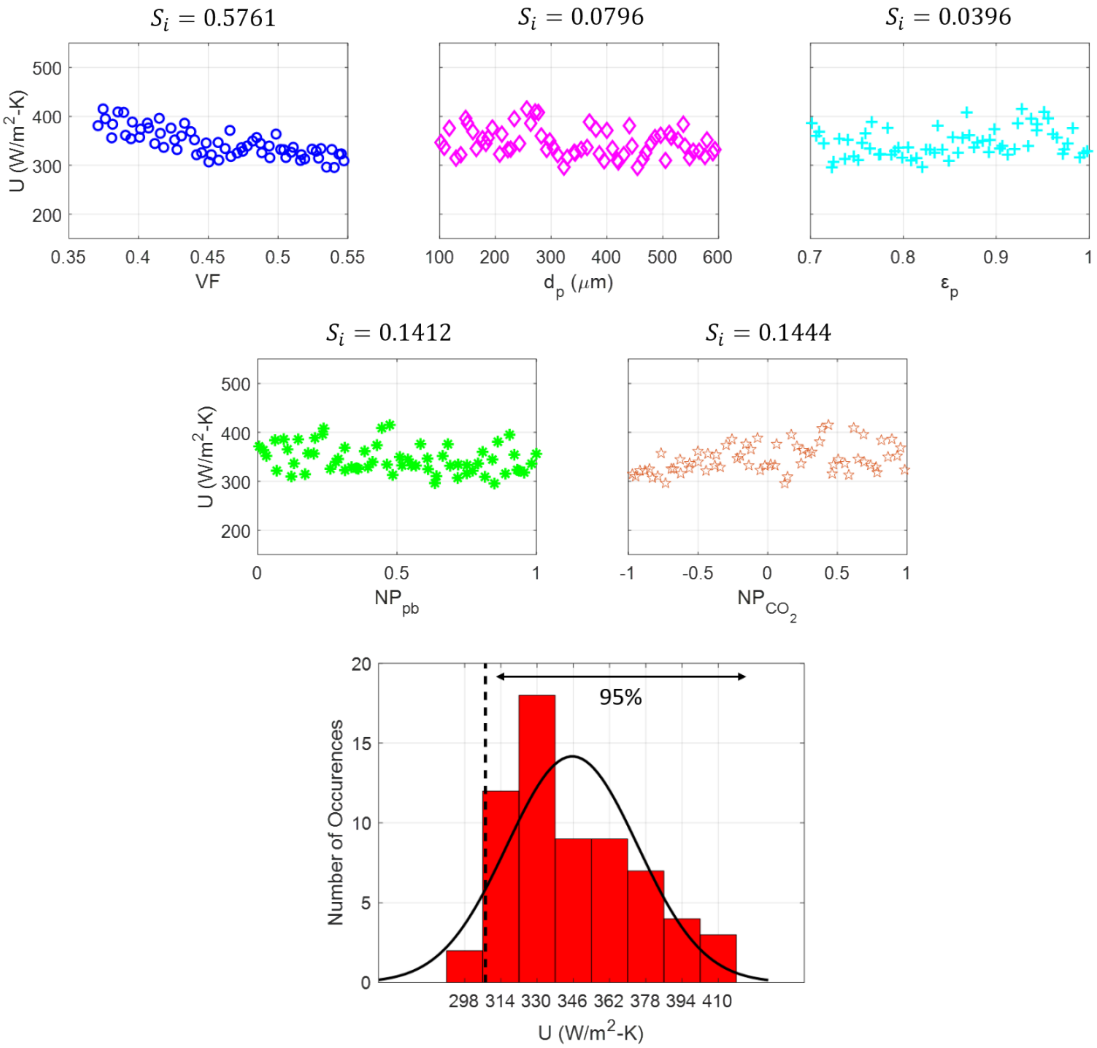

FIGURE 6. U vs sensitivity variables for reduced study w/ fixed geometric parameters.

aligning those overlapping regions of augmented flow is neither beneficial nor detrimental. It is important to emphasize that the range sampled for NP_{pb} and NP_{CO2} is rather arbitrary and was selected as an estimate of a worst-case flow maldistribution in a system. A well-designed system and functional heat exchanger will likely never experience those extreme values, and the sensitivity of those parameters would be far less pronounced.

The takeaway from this more targeted analysis is that of the variables that are less easily controlled or measured in a moving packed-bed heat exchanger, the void fraction has the highest sensitivity level. To reduce uncertainty in the model predictions, future efforts should focus on better characterizing the bed void fraction in a flowing state.

Discrete Element Modeling (DEM) can provide insight into the void fraction by modeling the particle-particle interaction as well as the particle interaction with the boundaries of the heat exchanger plate. This can be utilized in the design phase to minimize the void fraction, maximizing heat transfer. It can also be applied for existing heat exchangers to characterize spatial variations through flowing bed, which can then be integrated into the model to better resolve local thermal gradients. A potential limitation to using DEM, however, is that the solid mechanics models used for calculating the particle dynamics tend to be simplistic or require material properties that may be less understood than the void fraction itself. The sensitivity of the results to the specific model and the material properties would require some assessment to quantify the uncertainty.

Ideally the heat exchanger can be instrumented in a way that can measure the void fraction directly. Even if DEM modeling is successful those results would need to be verified experimentally. Various approaches have been used to measure the void fraction of a two-phase media. Visual techniques are most common, with many researchers utilizing high-speed imaging or laser diffraction techniques. Both of these options require optical access and therefore aren't viable for real-time measurements in the heat exchanger. A potential, albeit complex and expensive alternative is to use tomographical methods. Cross-sectional images of the flow through an opaque boundary can be taken using conventional CT and MRI machines, neither of which are realistic options for as a permanent fixture for taking repeated test measurements. Sardeshpande, Harinarayan, and Ranade [12] used electrical capacitance tomography (ECT) to measure void fractions in a two-phase air-water bubble flow and compared the results to conventional high-speed photography. ECT is a relatively new technology that shows promise for measuring dynamic void fractions in a high temperature opaque system. In the experiments conducted by the aforementioned researchers, an electrode ring was attached around the circumference of a column containing the flowing two-phase media. The capacitance is measured between pairs of electrodes, which are converted into permittivity values that can be converted to a spatial map. The permittivity of a dielectric can then be converted to a void fraction using established correlations. This type of technique would be particularly advantageous because it is non-intrusive, suitable for high temperatures, and relatively low cost. The authors emphasize that the technology is still very immature and underpredicts the void fraction by 40-50% when compared to data taken using conventional visual methods, so advances in the technology are required for this method to be a viable option.

CONCLUSIONS

A subscale moving packed-bed particle-to-sCO_2 heat exchanger was modeled to predict performance as a function of two geometric variables and five fluid-thermal variables. A sensitivity analysis was conducted and the Sobol indices were used to characterize the correlation between the overall heat transfer coefficient and each of the inputs. The results revealed that the overall performance of the heat exchanger is primarily correlated with the packed-bed channel width, which should be minimized while ensuring it is still sufficiently wide to prevent particle bridging. The analysis was performed again for a heat exchanger with fixed geometric parameters to isolate the sensitivity of the fluid-thermal variables. This study suggested that the performance of a heat exchanger in operation may still present a non-negligible amount of uncertainty despite having a fixed particle channel width. The majority of this variance is caused by uncertainty in the value of the packed-bed void fraction, a parameter which is difficult to characterize under flowing conditions. To reduce uncertainty in model predictions for moving packed-bed heat exchangers, potential options for experimental and computational characterization of the void fraction were discussed. Improved confidence in these models will reduce the level of overdesign of heat transfer surfaces that is currently required to mitigate risk and ensure the performance targets are met.

ACKNOWLEDGMENTS

This work was funded in part or whole by the U.S. Department of Energy Solar Energy Technologies Office under Award Number 34211 and 37371. This report was prepared as an account of work sponsored by an agency of the

 Sandia National Laboratories is a multimission laboratory managed and operated by National Technology & Engineering Solutions of Sandia, LLC, a wholly owned subsidiary of Honeywell International Inc., for the U.S. Department of Energy's National Nuclear Security Administration under contract DE-NA0003525.

REFERENCES

1. C.K. Ho, M. Carlson, K.J. Albrecht, Z. Ma, S. Jeter, and C.M. Nguyen, "Evaluation of Alternative Designs for a High Temperature Particle-to-sCO_2 Heat Exchanger," ASME. J. Sol. Energy Eng., 141(2): 021001 (2019).
2. K.J. Albrecht, M. Carlson, H. Laubscher, R. Crandell, N. DeLovato, and C.K. Ho, "Testing and Model Validation of a Prototype Moving Packed-Bed Particle-to-sCO2 Heat Exchanger," Proceedings of SolarPACES 2019, Daegu, South Korea, 2019.
3. K.J. Albrecht and C.K. Ho, "Design and Operating Considerations for a Shell-and-Plate, Moving Packed-Bed, Particle-to-sCO_2 Heat Exchanger," Solar Energy, vol. 178, pp. 331-340 (2019).
4. Sierra Thermal/Fluid Development Team, 2021, "SIERRA Multimechanics Module: Aria Thermal Theory Manual—Version 5.0," White Paper, Unlimited Release, Sandia National Laboratories, Albuquerque, NM, Report No. SAND2021-3922 695408.
5. A. Kruizenga, H. Li, M. Anderson, M. Corradini, "Supercritical Carbon Dioxide Heat Transfer in Horizontal Semicircular Channels," J. Heat Transfer, 134(8): 081802 (10 pages) (2012).
6. V. Gnielinski, "New Equations for Heat and Mass Transfer in Turbulent Pipe and Channel Flow," International Chemical Engineering, 16: 359-368 {1976).
7. Adams, B.M., et al. "Dakota, A Multilevel Parallel Object-Oriented Framework for Design Optimization, Parameter Estimation, Uncertainty Quantification, and Sensitivity Analysis: Version 6.14 User's Manual," Sandia Technical Report SAND2021-5822, May 2021. Updated
8. Le Pierres, R., Southall, D.; Osborne, S., "Impact of Mechanical Design Issues on Printed Circuit Heat Exchangers," Proceedings of SCO2 Power Cycle Symposium, University of Colorado at Boulder, CO, 2011.
9. An International Code - ASME Boiler & Pressure Vessel Code, Section II Part D (2019).
10. Zehner, P., Schlünder, E.U., 1970. Wärmeleitfähigkeit von Schüttungen bei mäβigen Temperaturen. Chemie Ingenieur Technik 42, 933–941.
11. A. Saltelli, P. Annoni, I. Azzini, F. Campolongo, M. Ratto, and S. Tarantola, "Variance based sensitivity analysis of model output. Design and estimator for the total sensitivity index," Computer Physics Communications, vol. 181, no. 2, pp. 259–270, Feb. 2010.
12. M. Sardeshpande, S. Harinarayan, and V. Ranade, "Void fraction measurement using Electrical Capacitance Tomography and High-Speed Photography," Chemical Engineering Research and Design, Vol 94, pp. 1-11 (2015).